

Screening for cocrystals of succinic acid and 4-aminobenzoic acid

Nizar Issa, Sarah A. Barnett, Sharmarke Mohamed, Doris E. Braun, Royston C. B. Copley, Derek A. Tocher, Sarah L Price*

Supplementary Information

Contents

1	Solubility of the ten APIs and two coformers.....	2
2	Infrared spectroscopy of the novel cocrystals.....	3
3	Summary of experimental screening results	5
4	Single crystal X-ray diffraction.....	6
4.1	Succinic acid • 2,2-bipyridine (I)	6
4.2	Succinic acid • diphencyclopropanone (II)	6
4.3	4-Aminobenzoic acid • antipyrine (III).....	7
4.4	4-Aminobenzoic acid • phenazine (IV).....	8
5	Computational.....	10
5.1	Conformational Analysis of succinic acid	10
5.2	Details of the lattice energy landscapes	12
5.2.1	Succinic acid	13
5.2.2	Dicyanobenzene	15
5.2.3	Bipyridine	16
5.2.4	Succinic acid•2,2'bipyridine cocrystal.....	17
5.2.5	Succinic acid•1,4-dicyanobenzene 1:1 cocrystal	18

1 Solubility of the ten APIs and two coformers

Table S1. Solubility measurements.

Compound	Soluble ^a	Partially soluble ^b	Practically insoluble ^c
4-Aminobenzoic acid	Acetone Acetonitrile Ethanol Ethyl acetate Methanol	Diethyl ether 1,4-Dioxane Nitromethane Water	
Succinic acid	Ethanol Ethyl acetate Methanol	Acetone Acetonitrile Diethyl ether 1,4-Dioxane, Water	Nitromethane
Metyrapone	Acetone 1,4-Dioxane Acetonitrile	Diethyl ether Ethanol Ethyl acetate Methanol	Nitromethane Water
β-Methyl-β-Nitrostyrene	Acetone Ethanol Ethyl Acetate Methanol	Acetonitrile Diethyl ether 1,4-Dioxane Nitromethane	Water
Bifonazole	Acetone 1,4-Dioxane Methanol	Acetonitrile Diethyl ether Ethanol Ethyl acetate	Nitromethane Water
1,4-Dicyanobenzene	Acetone Acetonitrile Methanol	1,4-Dioxane Ethanol	Diethyl ether Ethyl acetate Nitromethane Water
1-(5-Nitro-2-Pyridyl)Benzotriazole		Acetone Ethyl acetate Nitromethane Water	Acetonitrile Diethyl ether 1,4-Dioxane Ethanol Methanol
1-(2-Pyridyl)Benzotriazole	Acetone Ethyl Acetate	Acetonitrile Diethyl ether Ethanol Methanol	1,4-Dioxane Nitromethane Water
Phenazine	Acetone Diethyl ether 1,4-Dioxane	Acetonitrile Ethanol Ethyl acetate Methanol Nitromethane, Water	
Diphenylcyclopropenone	Acetone Acetonitrile 1,4-Dioxane Ethanol Ethyl acetate Methanol	Diethyl ether Nitromethane Water	
Antipyrine	Acetone Diethyl ether 1,4-Dioxane Ethanol Ethyl acetate Methanol	Nitromethane Water Acetonitrile	
2,2-Bipyridine	Acetone Acetonitrile Ethanol Ethyl acetate Methanol	Diethyl ether 1,4-Dioxane Nitromethane Water	

30 mg of the compound were placed in 10 mL of each of the nine solvent at room temperature and by visual evaluation the solvents were classified as ^asoluble: compound fully dissolved, ^bpartially soluble: some or most of the compound dissolved and ^cpractically insoluble: little or none of the compound dissolved.

2 Infrared spectroscopy of the novel cocrystals

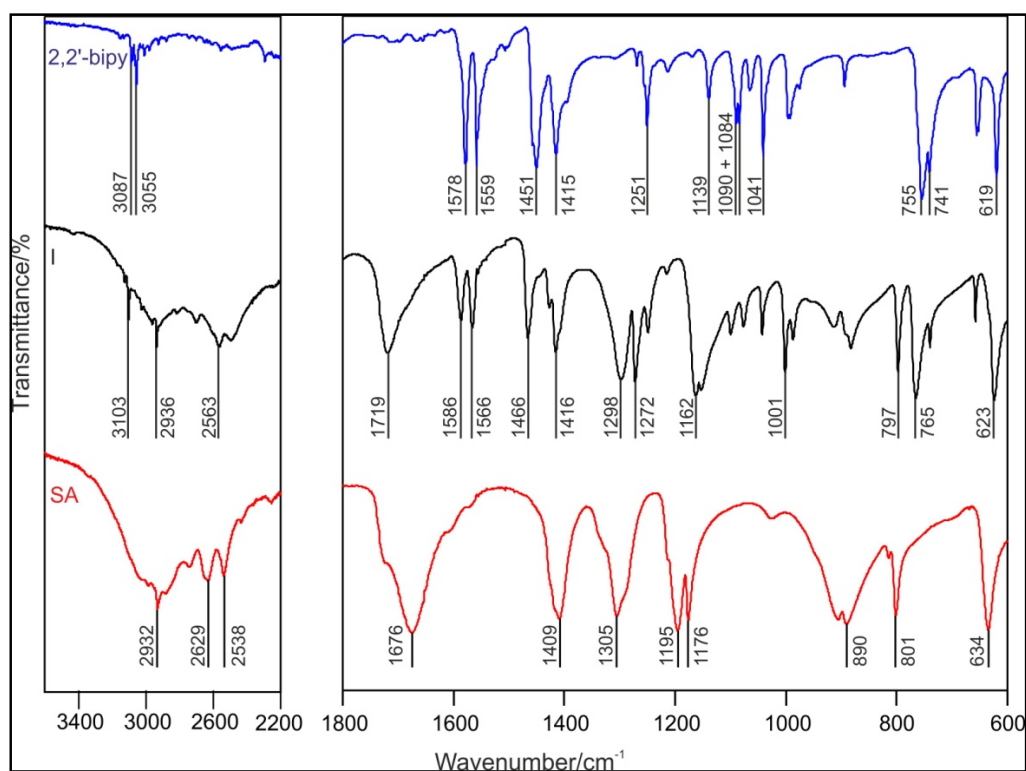


Figure S1. The IR spectra of 2,2'-bipyridine (blue), the cocrystal (I) produced by grinding (black), and β -succinic acid (red).

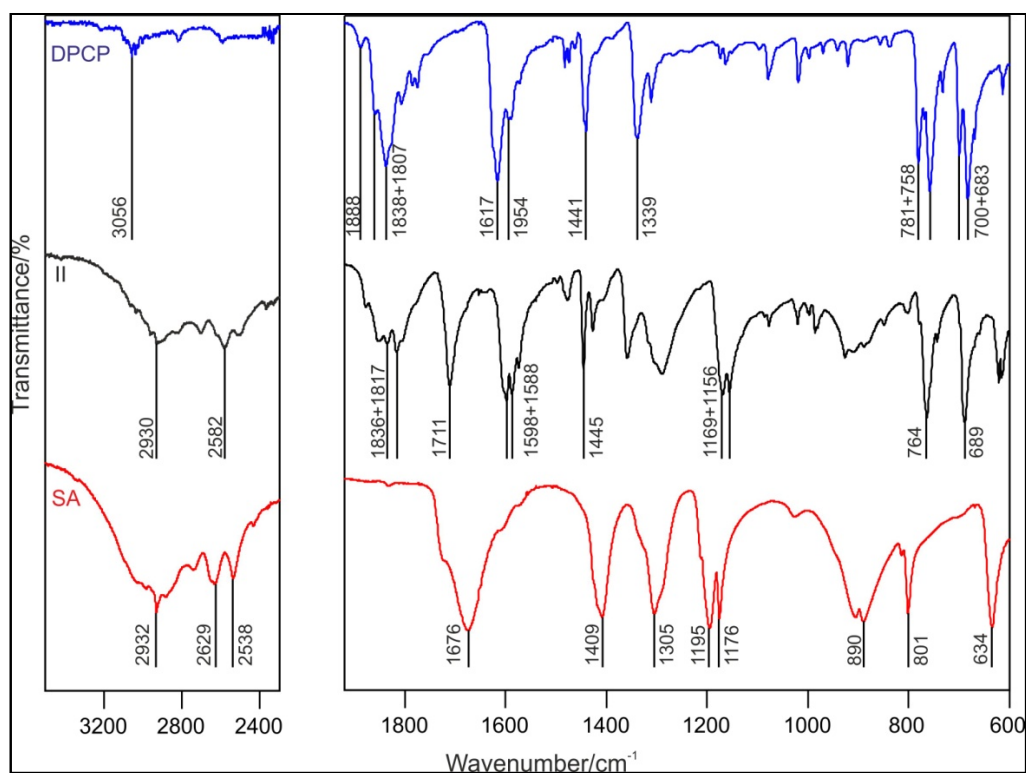


Figure S2. The IR spectra of diphenylcyclopropanone (blue), the cocrystal (II) produced by grinding (black), and β -succinic acid (red).

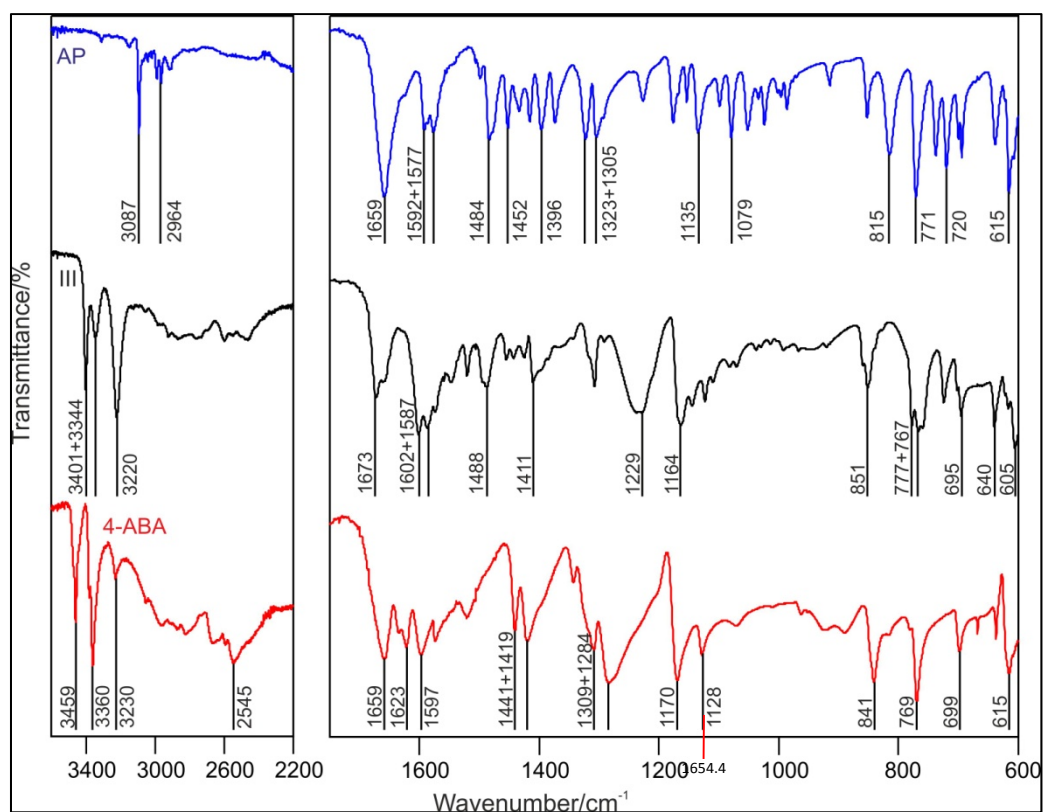


Figure S3. The IR spectra of antipyrine (blue), the cocrystal (III) produced by crystallization from amorphous III at 50 °C (black), and 4-aminobenzoic acid (red).

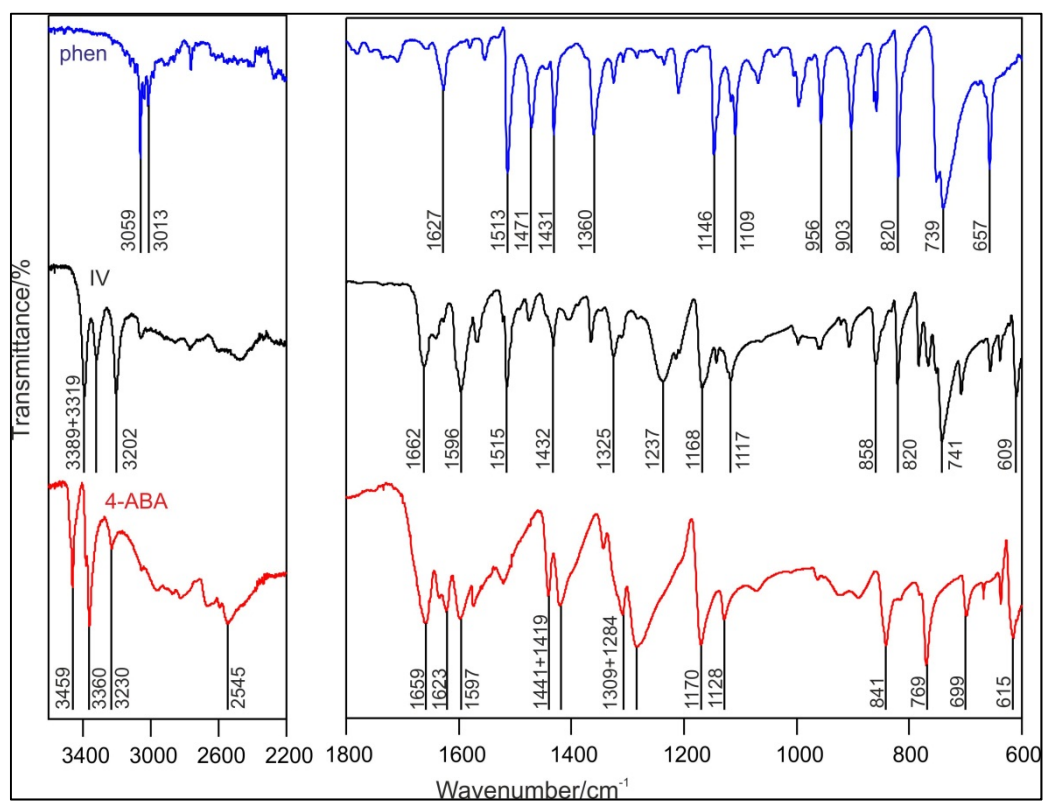


Figure S4. The IR spectra of phenazine (blue), the cocrystal (IV) produced by sublimation (black), and 4-aminobenzoic acid (red).

3 Summary of experimental screening results

Table S2. Overview of experimental screening results. The cocrystals with published single crystal structures which had been grown from solvents are indicated in bold and the CSD code given.

Cocrystallizing agent	Biological building block	Stage I Indication of cocrystallization:			Stage II
		Neat grinding	Solvent assisted grinding	HSM	Single crystals of:
Succinic acid	Metirapone	×	×	-	×
	β-Methyl-β-Nitrostyrene	×	×	-	β-Methyl-β-Nitrostyrene
	Bifonazole	×	×	×	Bifonazole
	1,4-Dicyanobenzene	×	×	×	1,4-Dicyanobenzene
	1-(5-Nitro-2-Pyridyl)Benzotriazole	×	×	×	×
	1-(2-Pyridyl)Benzotriazole	×	×	×	×
	Phenazine	×	✓	✓	WOQBOT
	Diphenylcyclopropanone	✓	✓	✓	Succinic acid • diphenylcyclopropanone (II)
	Antipyrine	×	×	×	×
	2,2'-Bipyridine	×	✓	✓	Succinic acid • 2,2'-bipyridine (I)
4-Aminobenzoic acid	Metirapone	×	×	-	×
	β-Methyl-β-Nitrostyrene	×	×	-	×
	Bifonazole	×	×	×	Bifonazole
	1,4-Dicyanobenzene	×	×	×	1,4-Dicyanobenzene
	1-(5-Nitro-2-Pyridyl)Benzotriazole	×	×	×	×
	1-(2-Pyridyl)Benzotriazole	×	×	×	×
	Phenazine	×	✓	✓	4-Aminobenzoic acid • phenazine (IV)
	Diphenylcyclopropanone	×	×	×	×
	Antipyrine	✓	✓	✓	4-Aminobenzoic acid • antipyrine (III)
	2,2'-Bipyridine	×	✓	-	DAQYUQ

✓: cocrystal formation, ×: no cocrystal formation observed, -: not attempted, as large melting point difference.

4 Single crystal X-ray diffraction

4.1 Succinic acid•2,2'-bipyridine (I)

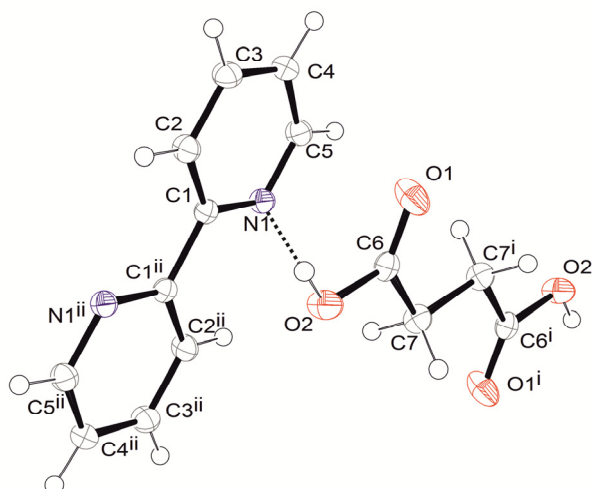


Figure S5. Thermal ellipsoid plots of succinic acid•2,2'-bipyridine (I). Displacement ellipsoids are drawn at the 50% probability level. Atoms generated by inversion labelled with i and ii.

Table S3. Geometrical parameters for intermolecular interactions in I.

$D-H\cdots A$	$D-H$ (Å)	$H\cdots A$ (Å)	$D\cdots A$ (Å)	$D-H\cdots A$ (°)
$O2-H1\cdots N1^i$	0.91(2)	1.87(2)	2.7774(14)	177(2)

Symmetry code: (i) $x, y-1, z$.

4.2 Succinic acid•diphenylcyclopropenone (II)

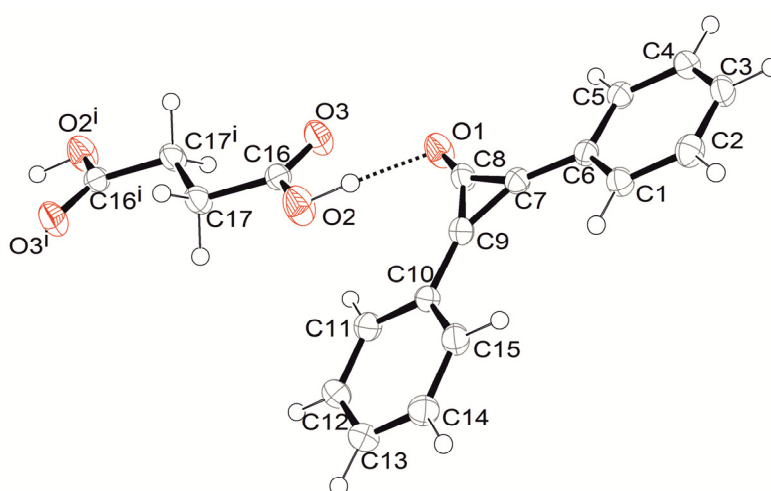


Figure S6. Thermal ellipsoid plots of succinic acid • diphenylcyclopropenone (II). Displacement ellipsoids are drawn at the 50% probability level. Atoms generated by inversion labelled with i.

Table S4. Geometrical parameters for intermolecular interactions in II.

<i>D</i> —H··· <i>A</i>	<i>D</i> —H (Å)	H··· <i>A</i> (Å)	<i>D</i> ··· <i>A</i> (Å)	<i>D</i> —H··· <i>A</i> (°)
O2—H11···O1 ⁱ	0.96 (3)	1.68 (3)	2.6351 (15)	170 (2)

Symmetry code: (i) *x*, $-y+3/2$, $z+1/2$.

4.3 4-Aminobenzoic acid•antipyrine (III)

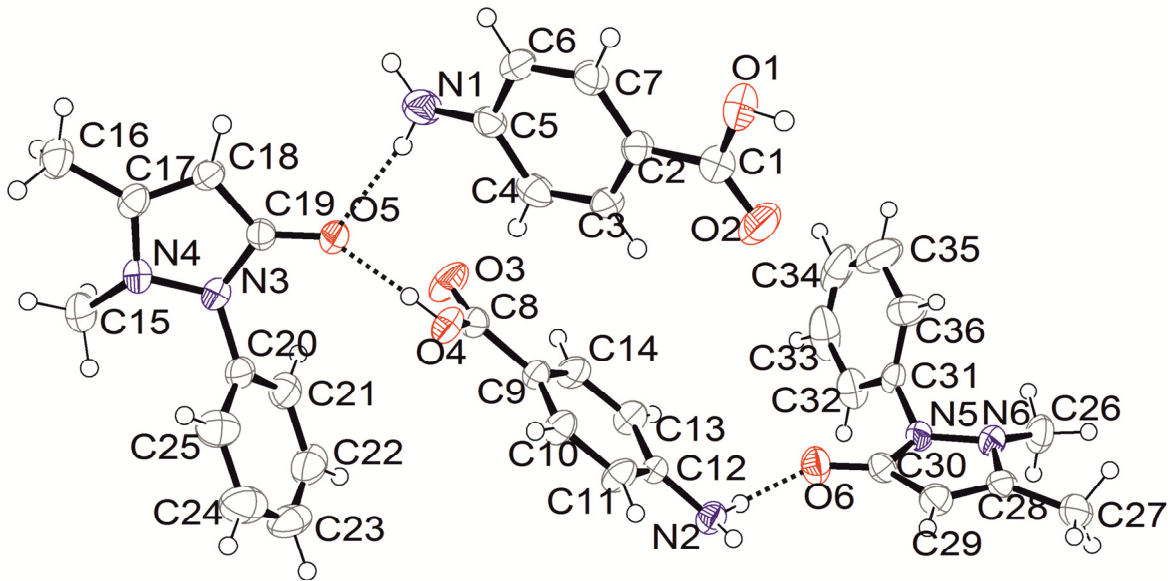


Figure S7. Asymmetric unit of 4-aminobenzoic acid•antipyrine (III). Displacement ellipsoids are drawn at the 50 % probability level.

Table S5. Geometrical parameters for intermolecular interactions in III.

<i>D</i> —H··· <i>A</i>	<i>D</i> —H (Å)	H··· <i>A</i> (Å)	<i>D</i> ··· <i>A</i> (Å)	<i>D</i> —H··· <i>A</i> (°)
N1—H4···O5	0.81 (4)	2.14 (4)	2.946 (4)	170 (3)
N1—H5···O3 ⁱ	0.92 (4)	2.18 (4)	3.065 (4)	163 (3)
N2—H11···O2 ⁱⁱ	0.85 (3)	2.08 (3)	2.923 (4)	171 (3)
N2—H12···O6 ⁱⁱⁱ	0.89 (3)	2.09 (4)	2.971 (4)	173 (3)
O1—H1···O6 ^{iv}	0.852(10)	1.752(12)	2.598 (3)	172 (4)
O4—H8···O5	0.84(3)	1.78(4)	2.597 (3)	164 (4)

Symmetry codes: (i) $-x+1$, $y-1/2$, $-z+2$; (ii) $-x+2$, $y+1/2$, $-z+1$; (iii) $x+1$, y , z ; (iv) $x+1$, $y-1$, z .

4.4 4-Aminobenzoic acid•phenazine (IV)

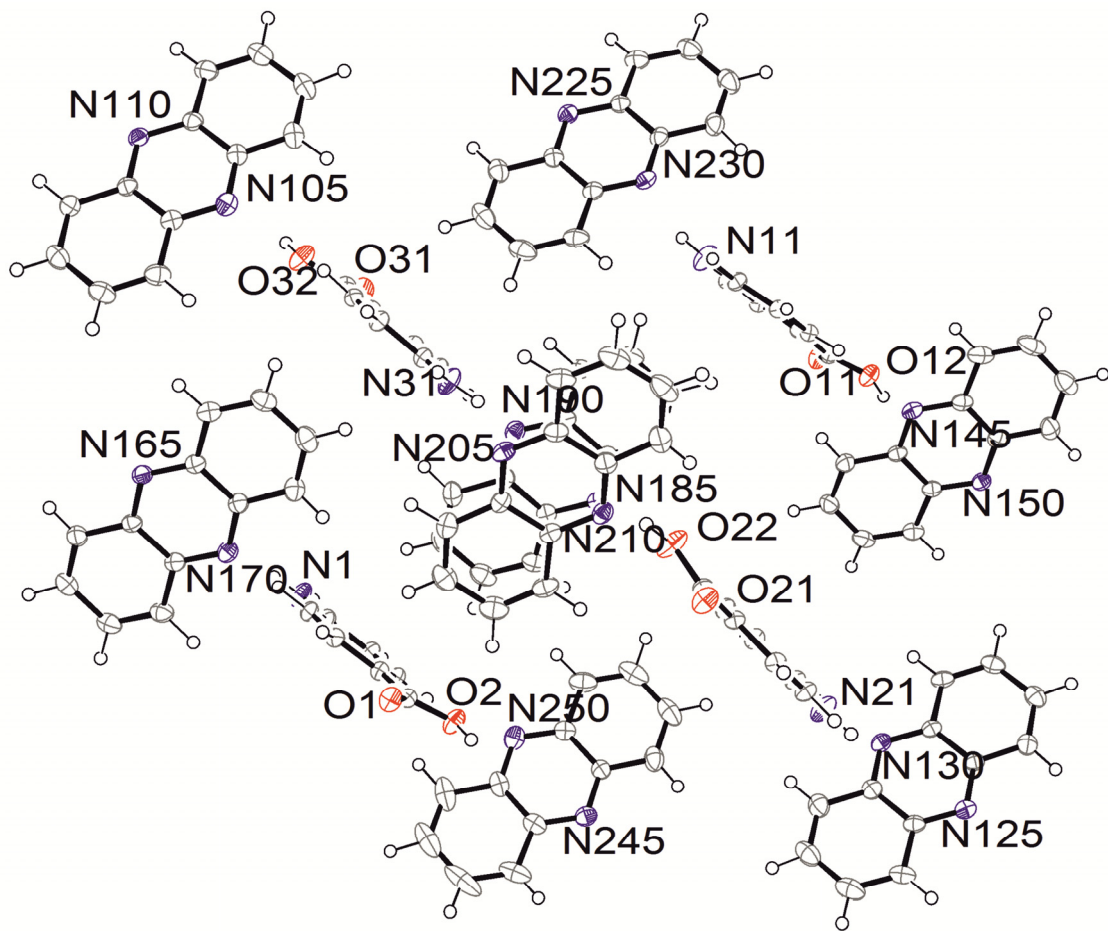


Figure S8. Asymmetric unit of 4-aminobenzoic acid•Phenazine (IV). Displacement ellipsoids are drawn at the 50 % probability level. Hydrogen bonds are omitted for clarity.

Table S6. Geometrical parameters for intermolecular interactions in IV.

<i>D</i> —H··· <i>A</i>	<i>D</i> —H (Å)	H··· <i>A</i> (Å)	<i>D</i> ··· <i>A</i> (Å)	<i>D</i> —H··· <i>A</i> (°)
N1—H1B···O11 ⁱ	0.94 (2)	1.98 (2)	2.894 (2)	165 (2)
N1—H1A···N165 ⁱⁱ	0.85 (2)	2.18 (2)	3.034 (2)	176 (2)
N11—H11A···O1 ⁱⁱⁱ	0.89 (2)	2.04 (2)	2.919 (2)	170 (2)
N11—H11B···N245 ^{iv}	0.90 (2)	2.16 (2)	3.055 (2)	173 (2)
N21—H21A···O31 ⁱⁱⁱ	0.90 (2)	2.00 (2)	2.8827 (19)	167.4 (19)
N21—H21B···N110 ^v	0.93 (2)	2.15 (2)	3.057 (2)	166 (2)
N31—H31A···N185 ⁱⁱⁱ	0.86 (3)	2.17 (3)	3.025 (2)	173 (2)
N31—H31B···O21 ^{vi}	0.92 (2)	2.00 (2)	2.902 (2)	165 (2)
O2—H2A···N225 ^{vii}	0.96 (3)	1.76 (3)	2.6873 (18)	161 (2)
O12—H12A···N150 ^{viii}	0.99 (3)	1.75 (3)	2.7112 (19)	161 (3)
O22—H22A···N205 ^{vi}	1.02 (3)	1.71 (3)	2.7061 (19)	163 (3)
O32—H32A···N125 ^{ix}	0.97 (3)	1.76 (3)	2.7036 (18)	163 (3)

Symmetry codes: (i) $-x+2, -y+1, -z+1$; (ii) $-x+1, -y+1, -z$; (iii) $-x+1, -y+1, -z+1$; (iv) $x, y+1, z$; (v) $x, y-1, z+1$; (vi) $-x, -y+1, -z+1$; (vii) $x, y-1, z$; (viii) $-x+2, -y+1, -z+2$; (ix) $x, y+1, z-1$.

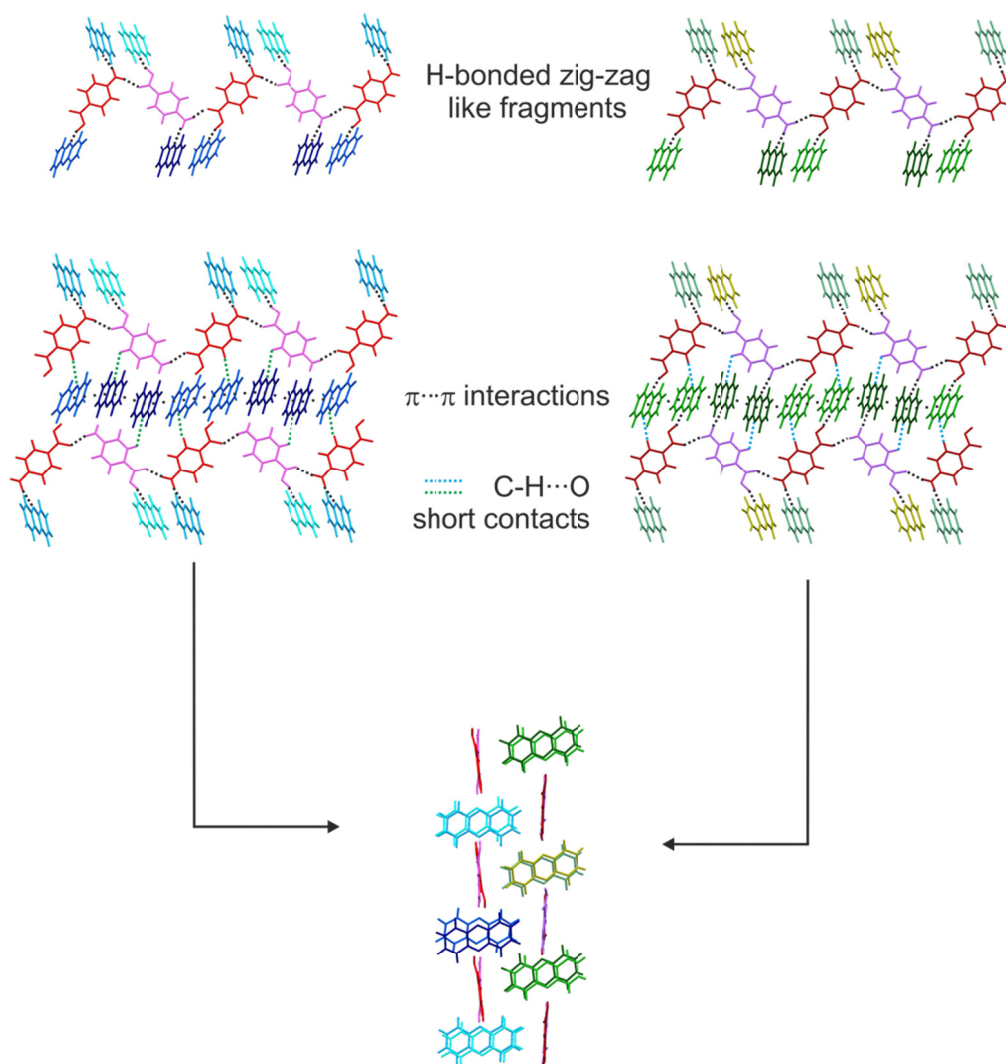


Figure S9. Packing diagram for 4-ABA•phenazine (IV) showing the two crystallographically distinct zig-zag like fragments, the interactions in between each of the two distinct sheets, and the stacking of the two sheets. Independent molecules are coded by shades of colour.

5 Computational

5.1 Conformational Analysis of succinic acid

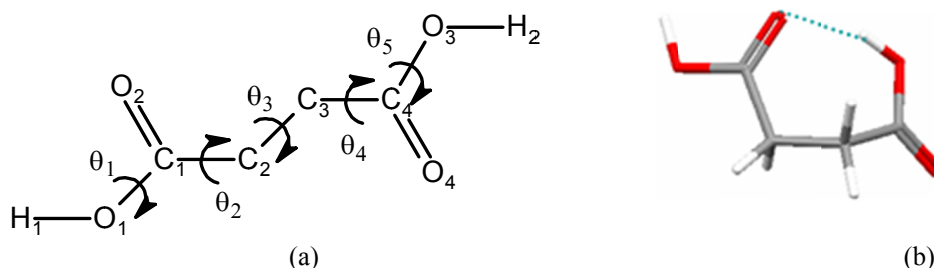


Figure S10. (a) The five torsion angles of succinic acid. The molecule is depicted in the planar conformation with $\theta_1 = \text{H}_1\text{O}_1\text{C}_1\text{C}_2 = 180^\circ$, $\theta_2 = \text{O}_1\text{C}_1\text{C}_2\text{C}_3 = 180^\circ$, $\theta_3 = \text{C}_1\text{C}_2\text{C}_3\text{C}_4 = 180^\circ$, $\theta_4 = \text{O}_3\text{C}_4\text{C}_3\text{C}_2 = -180^\circ$ and $\theta_5 = \text{H}_2\text{O}_3\text{C}_4\text{C}_3 = -180^\circ$. For clarity the hydrogen atoms on the carbon chain are not shown. (b) A local minimum in the conformational energy of succinic acid with an intramolecular hydrogen bond.

Succinic acid (SA) has 5 torsion angles (Figure S10a) that may vary in crystal structures, though θ_1 and θ_5 as well as θ_2 and θ_4 are symmetry related in the gas phase and in many crystals. The CSD (Version 1.11, Nov 08) was used to search for structures that contained neutral SA, whose coordinates are fully determined with no disorder and an R-factor $\leq 10\%$. If multiple entries of the same structure in the CSD existed, the one with the lowest R-factor determined at the lowest temperature, with a preference for any neutron determinations was used. In total 56 experimental structures containing succinic acid were found, which, given that some had more than one succinic acid in the asymmetric unit, gave a total 62 inequivalent neutral succinic acid conformations in crystal structures, which were analyzed using Vista.

The conformational minima for the isolated molecule were determined at the MP2/631G(d,p) level of theory, using GAUSSIAN03, following various scans of the conformational potential energy surface. The global minimum conformation was non-planar, with $\theta_3 = -66.1^\circ$. Hence Figure S11 depicts two sections of the conformational energy surface for varying the carboxylic acid torsions θ_2 and θ_4 , one corresponding $\theta_3 = -66.1^\circ$ and the other for a planar conformation $\theta_3 = 180^\circ$. Since all succinic acid molecules in the crystal structures had either $57^\circ < |\theta_3| < 72^\circ$ or $170^\circ < |\theta_3| < 180^\circ$ torsion angles, their conformations could be represented on Figure S11. The only local minima in the conformational energy surface which is not shown schematically on Figure S11 is an internally hydrogen bonded conformation shown in Figure S10b.

The overwhelming majority of the succinic acid molecules in the crystalline environment, 50/62 are approximately planar in Conf A, close to the local energy minima (Figure S11a and Table S15). The majority of cases where the succinic conformation is not Conf A, appears to correlate with the other molecules in the crystal structure having a complex structure with multiple hydrogen bond donor/acceptor groups located so that there are severe steric restrictions on forming hydrogen bonds with a planar (Conf A) succinic acid molecule. The molecules in WOJHEI and JAZBES adopt the high energy planar conformation with the carboxylic acid groups rotated (Conf B) in order to form the hydrogen bonds. The succinic acid is non-planar in Conf C, approximating the most stable gas phase structure, in JEDLAG01, QEVMEJ and SERMOR10, and in Conf. E, the related local energy minimum, in CIRXAD, JEKDUY, KIJSEC, KTHSUC, OLOFUQ and one molecule of PEKQOM. The only structure not close to a freely optimised conformation is the second molecule in PEKQOM, which approximates Conf D (Figure S11b) enabling it to form hydrogen bonds with 4 partner molecules.

Table S7. Freely optimized conformations of succinic acid and their frequency of occurrence in experimental crystal structures.

Conformation	$\Delta\text{MP2}^{\text{a}}$ (kJ/mol)	$\Delta\text{HF}^{\text{b}}$ (kJ/mol)	θ_3	θ_2	θ_4	θ_1	θ_5	Crystal structures ^c
Conf C	-	-	-66.01	170.30	170.21	179.54	179.55	3
Conf E	5.60	8.10	-59.28	-178.64	-31.23	179.47	179.66	6
Conf A	6.37	1.86	177.29	177.13	177.06	179.56	179.56	50
Intramolecular H-bond	15.77	20.06	-79.59	-168.66	69.02	-178.93	-1.47	0
Conf B	17.82	21.10	178.94	1.94	56.37	179.97	-179.92	2

^aThe energies, relative to Conf C, of these structures, freely optimised at the MP2 6-31G(d,p) level of theory. ^bThe relative SCF component of this energy. ^cThe number of succinic acid molecules in crystal structures which approximate this conformation. Only one molecule is too far from any of these structures to be included (see Conf D region on Fig. S11(b) for this structure and Figs. 11 spread of structures in each conformational class).

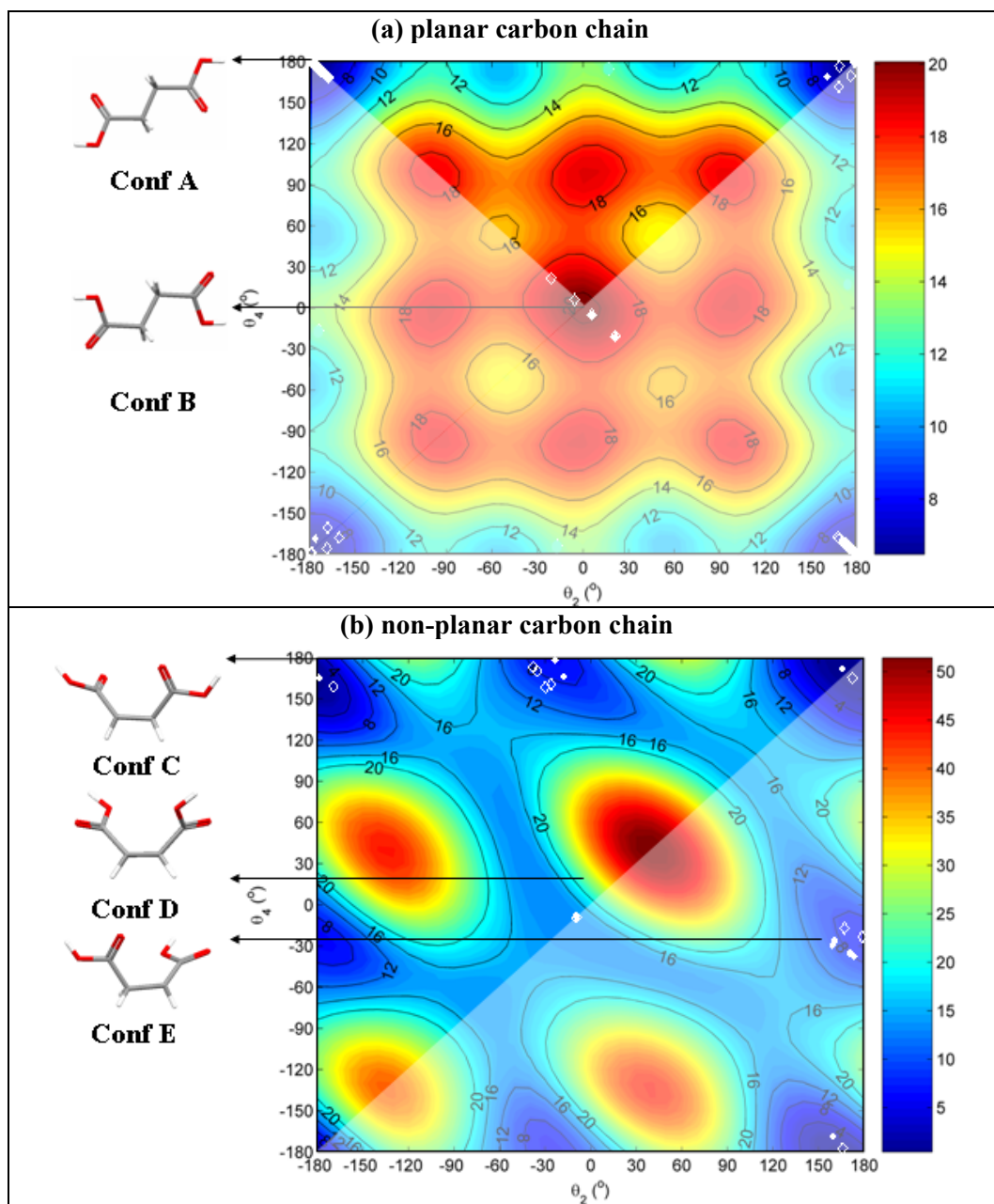


Figure S11. MP2/6-31G(d,p) relaxed intramolecular energy (kJ mol^{-1}) scans for succinic acid as a function of rotation about the two carboxylic acid groups, for (a) the planar conformation with the carbon chain torsion ($\theta_3 = \text{C}_1\text{-C}_2\text{-C}_3\text{-C}_4$) constrained to 180° and (b) with $\theta_3 = \text{C}_1\text{-C}_2\text{-C}_3\text{-C}_4$ constrained to -66.1° . In both scans the carboxylic acid groups were constrained to the planar geometry. The molecular symmetry of the isolated molecule is represented by shading the symmetry equivalent areas. The conformations observed in crystal structures are shown by full diamonds for the conformation observed in the CSD as generated by the program Vista, with open diamonds denoting the symmetry equivalent conformations.

5.2 Details of the lattice energy landscapes

The following lattice energy landscapes show two levels of accuracy in evaluating the relative lattice energies and refining the crystal structures. The lattice energy landscape for

each search shows all the low energy crystal structures found by treating the molecule structures as rigid in the MP2/6-31G(d,p) optimised isolated molecule conformation. In this approximation, the lattice energy is just the intermolecular lattice energy, U_{inter} , calculated with a distributed multipole electrostatic model and the FIT repulsion-dispersion potential. The lower energy structures were further refined by allowing specified torsion angles (see m/s Table 1) to respond to the packing forces, by optimising $E_{\text{latt}}=U_{\text{inter}}+\Delta E_{\text{intra}}$, where ΔE_{intra} , is the MP2/6-31G(d,p) energy penalty for the change in conformation. The resulting minima are also shown, joined to the starting rigid-body structure, indicating the lowering in lattice energy that results from considering this conformational flexibility. All the experimental crystal structures are compared with the nearest structure found in the search after optimising $E_{\text{latt}}=U_{\text{inter}}+\Delta E_{\text{intra}}$ in Table S8.

5.2.1 Succinic acid

The succinic acid crystal energy landscape is divided into the $Z'=1$ search (Figure S12a), for comparability with the other searches and a $Z'=2$ search (Figure S12b) to test whether the methodology could find the metastable α polymorph. The stable β form is the global minimum on the lattice energy landscape, but there are several alternative packings of the $R_2^2(8)$ carboxylic acid chain motif that are more stable than the observed metastable polymorph. This may reflect the poorer reproduction of the structure of the α polymorph (Table S16). Non-planar conformations gave rise to crystal structures that were so much less dense than those generated with the planar conformation that they required a separate plot (Figure S13a) and seem unlikely to be feasible polymorphs.

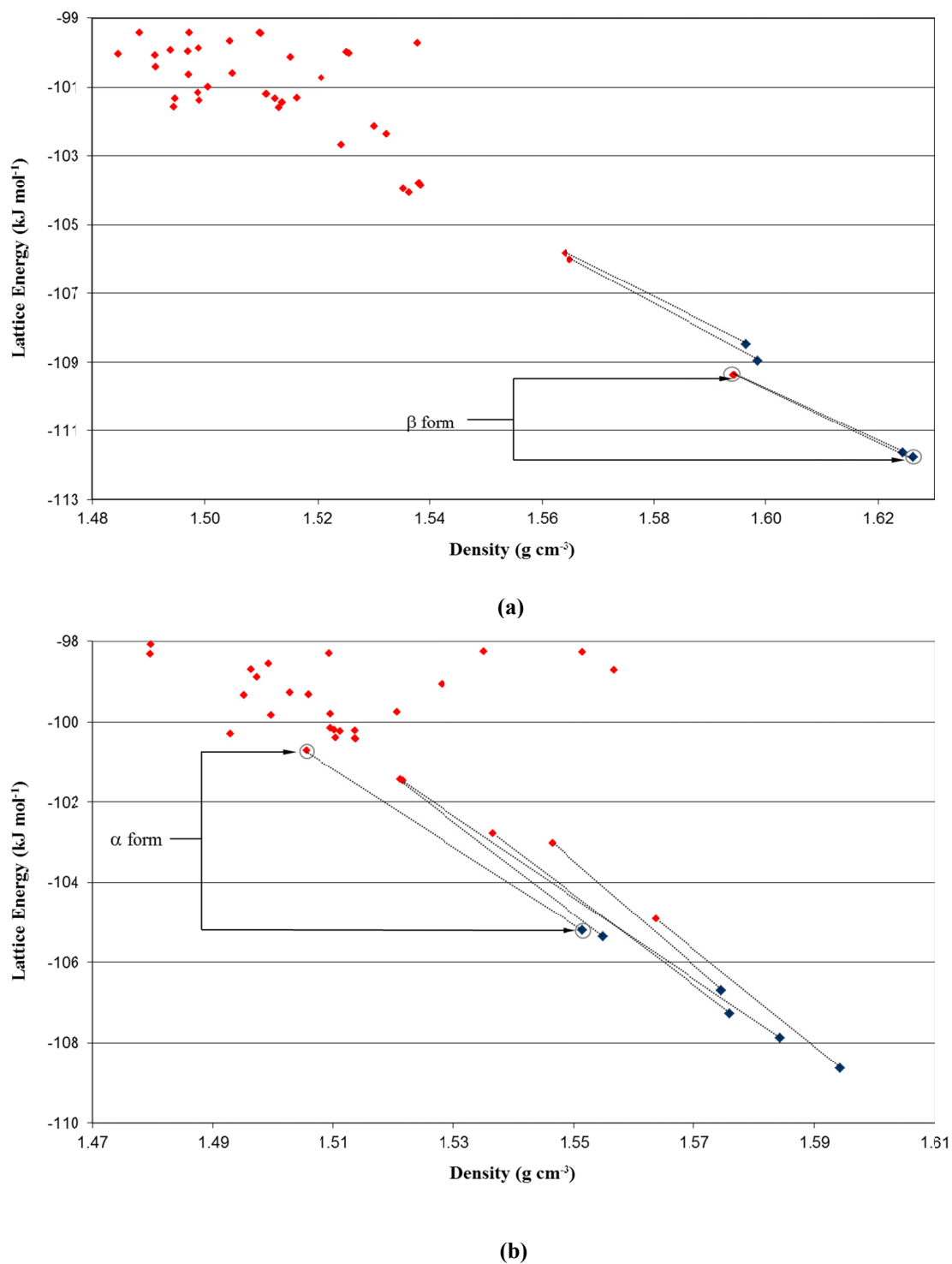


Figure S12. Lattice energy landscapes for succinic acid for a search of (a) $Z'=1$ structures and (b) $Z'=2$ search structures using Conf A. The red symbols indicate energy minima obtained after the rigid body search, which are connected by dashed lines to the corresponding minima (blue symbols), when the 5 torsion angles are allowed to change in response to the intermolecular forces. The open circles denote the corresponding minima starting from the experimental structures.

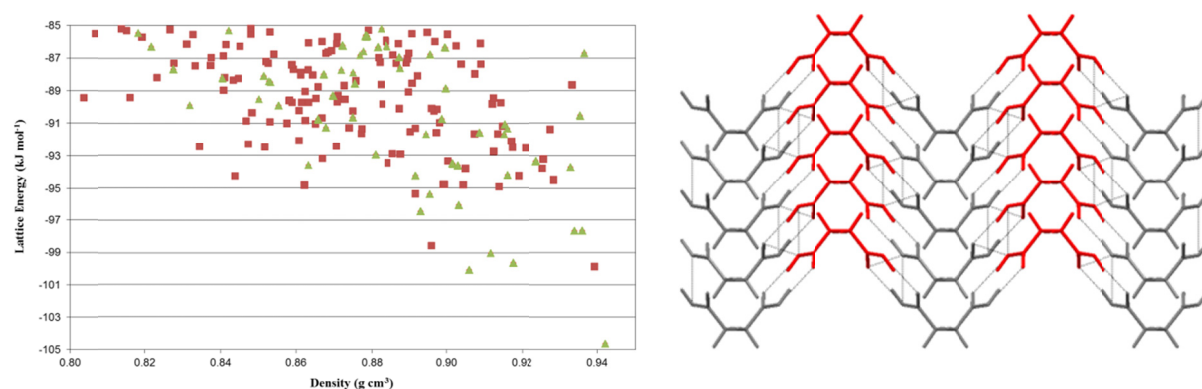


Figure S13. Hypothetical crystal structures for non-planar succinic acid. (a) Lattice energy landscape generated for the non-planar conformations **Conf C** and **Conf E** of succinic acid. (b) The ribbon motifs of the global minimum structure with the non-planar conformation C of succinic acid.

5.2.2 1,4-Dicyanobenzene

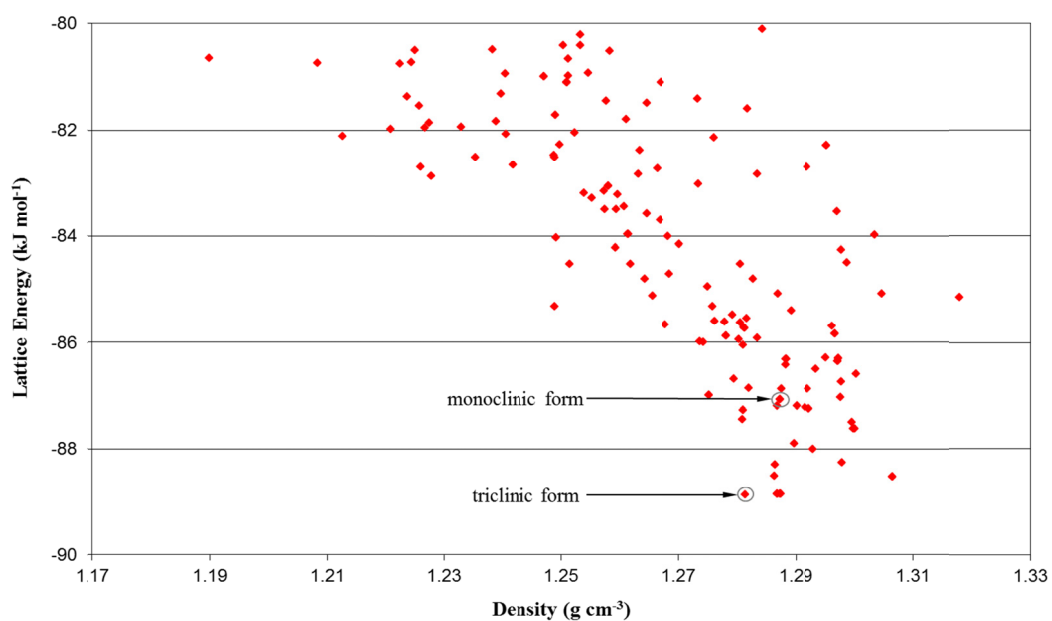


Figure S14. Lattice energy landscape for 1,4-dicyanobenzene. The red symbols indicate lattice energy minima obtained after the rigid body and the open circles denote the known experimental structures.

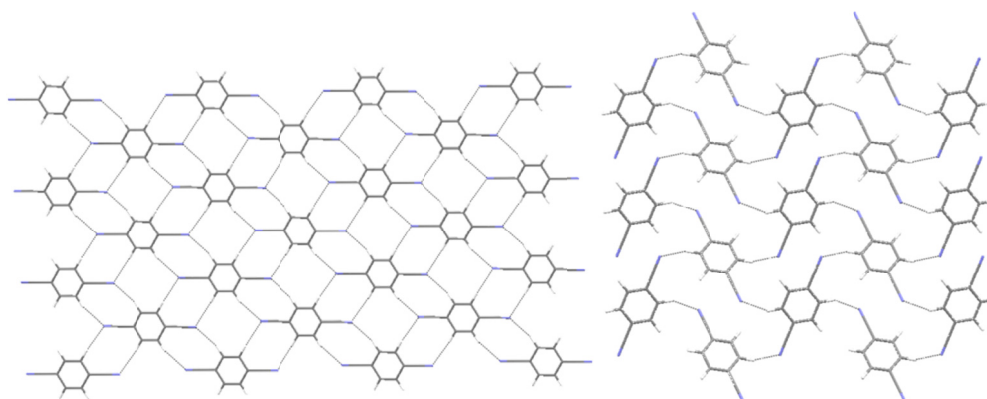


Figure S15. Packing motifs of 1,4-dicyanobenzene polymorphs (left) ribbon type motif observed for the triclinic structure and (right) ladder type motif observed for the monoclinic structure. These motifs are seen in the other low energy structures.

5.2.3 2,2'-Bipyridine

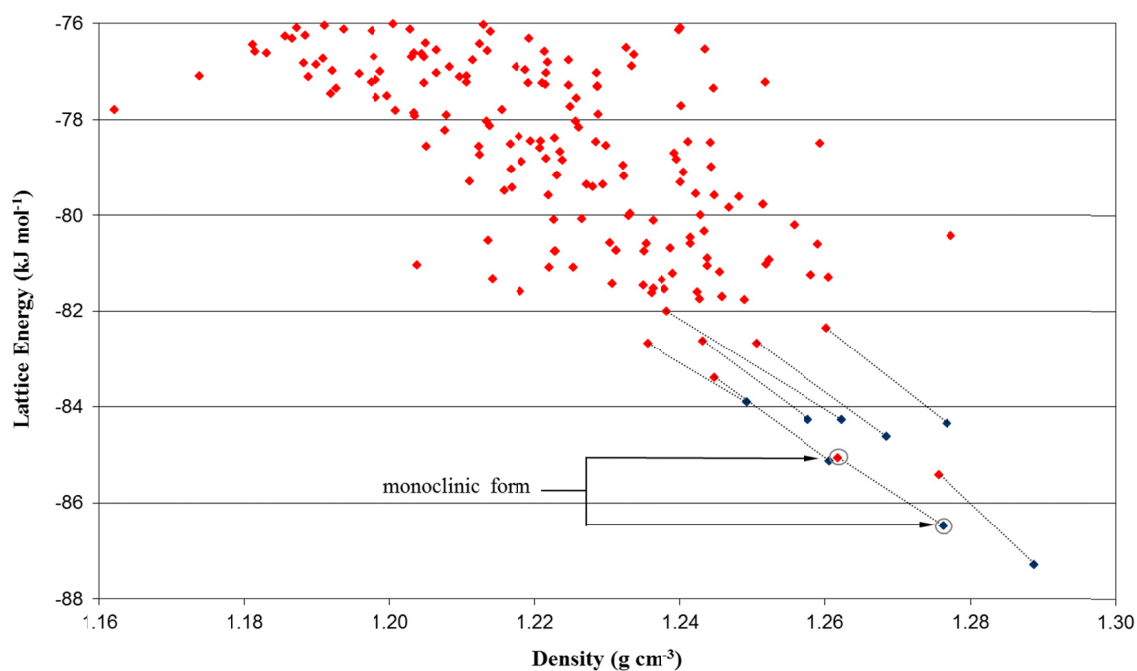


Figure S16. Lattice energy landscape for 2,2'-bipyridine. The red symbols indicate energy minima obtained after the rigid body search, which are connected by dashed lines to the corresponding minima, blue symbols, when the central torsion angle is allowed to change in response to the intermolecular forces. The open circles denote the corresponding minima starting from the experimental structure.

5.2.4 Succinic acid•2,2'-bipyridine cocrystal

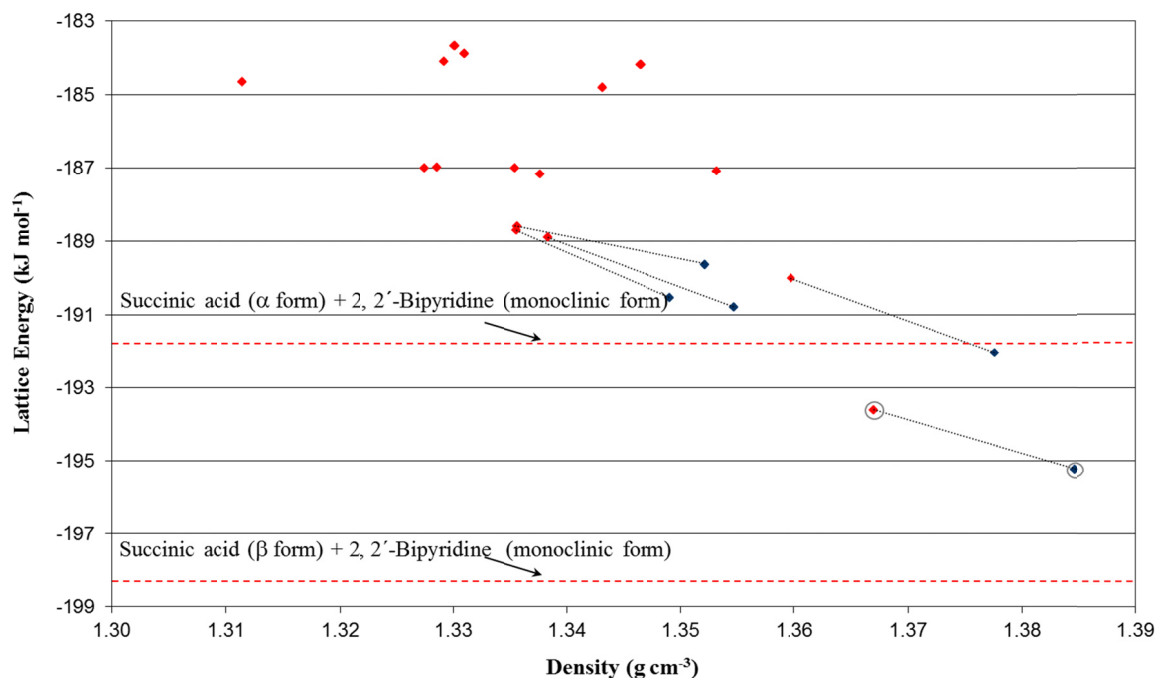


Figure S17. Lattice energy landscape for 1:1 cocrystals of succinic acid•2,2'-bipyridine. The red symbols indicate energy minima obtained after the rigid body search, which are connected by dashed lines to the corresponding minima, blue symbols, when the 5 succinic acid and 1 bipyridine torsion angles are allowed to change in response to the intermolecular forces. The open circles denote the corresponding minima starting from the experimental structure. The red dashed lines indicate the sum of the lattice energies for the pure components.

5.2.5 Succinic acid•1,4-dicyanobenzene 1:1 cocrystal

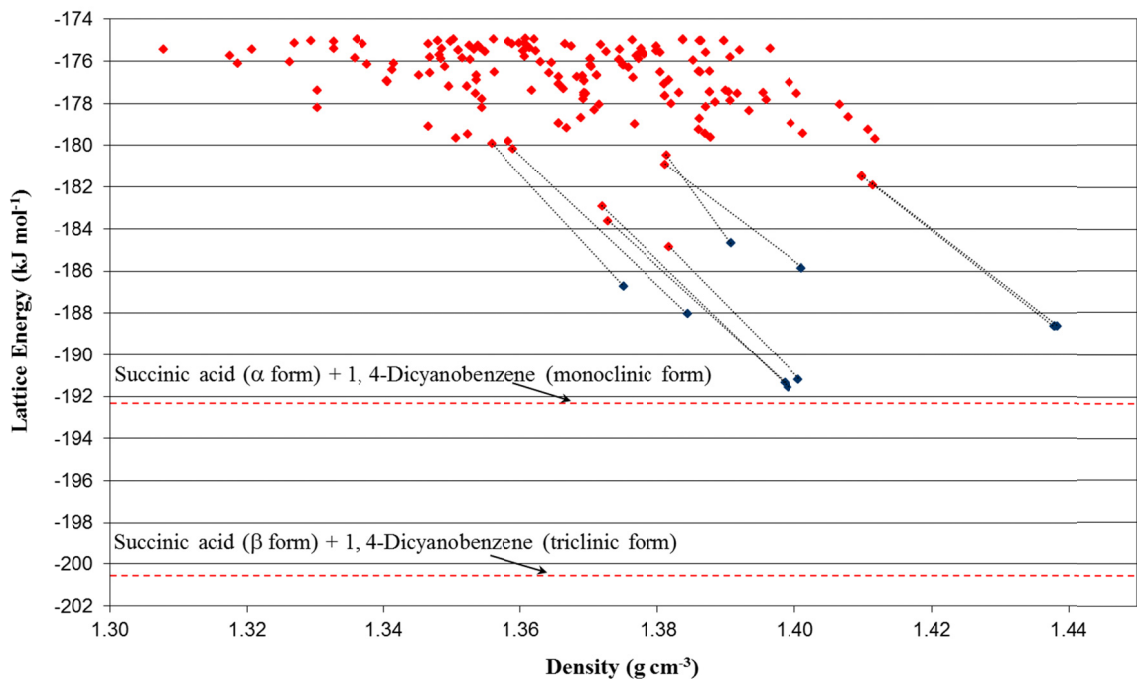


Figure S18. Lattice energy landscape for the hypothetical cocrystal of succinic acid•1,4-dicyanobenzene. The red symbols indicate energy minima obtained after the rigid body search, which are connected by dashed lines to the corresponding minima, blue symbols, when the 5 succinic acid torsion angles are allowed to change in response to the intermolecular forces. The red dashed lines indicate the sum of the lattice energies for the pure components.

Table S8. Comparison of structures found in the searches with the experimental crystal structures.

	a / Å	b / Å	c / Å	α / °	β / °	γ / °	Density / g cm ⁻³	E _{latt} / kJ/mol	RMSD ₁₅ / Å
Succinic Acid									
Expt α <i>P</i> -1	5.727	6.867	7.198	101.84	109.10	97.18	1.531		
Calc	5.983	6.515	7.282	101.80	109.69	99.74	1.551	-105.19	0.30
Expt β <i>P</i> ₂ ₁ /c	5.526	8.881	5.105		91.49		1.566		
Calc	5.392	8.707	5.147		93.49		1.626	-111.78	0.20
1,4-dicyanobenzene									
Expt <i>P</i> ₂ ₁	3.868	7.080	12.127		97.21		1.291		
Calc	3.755	7.356	12.163		100.27		1.287	-87.08	0.30
Expt <i>P</i> -1	3.847	6.585	7.322	114.50	93.60	96.90	1.279		
Calc	3.654	6.660	7.651	113.96	95.67	97.88	1.281	-88.87	0.34
2,2'-bipyridine									
Expt <i>P</i> ₂ ₁ /c	5.486	6.165	12.376		110.92		1.326		
Calc	5.656	6.264	12.318		111.36		1.276	86.48	0.16
2,2'-bipyridine•succinic acid cocrystal									
Expt <i>P</i> ₂ ₁ /c	8.958	5.178	14.357		106.11		1.423		
Calc	9.423	5.132	14.089		105.06		1.385	-195.23	0.25

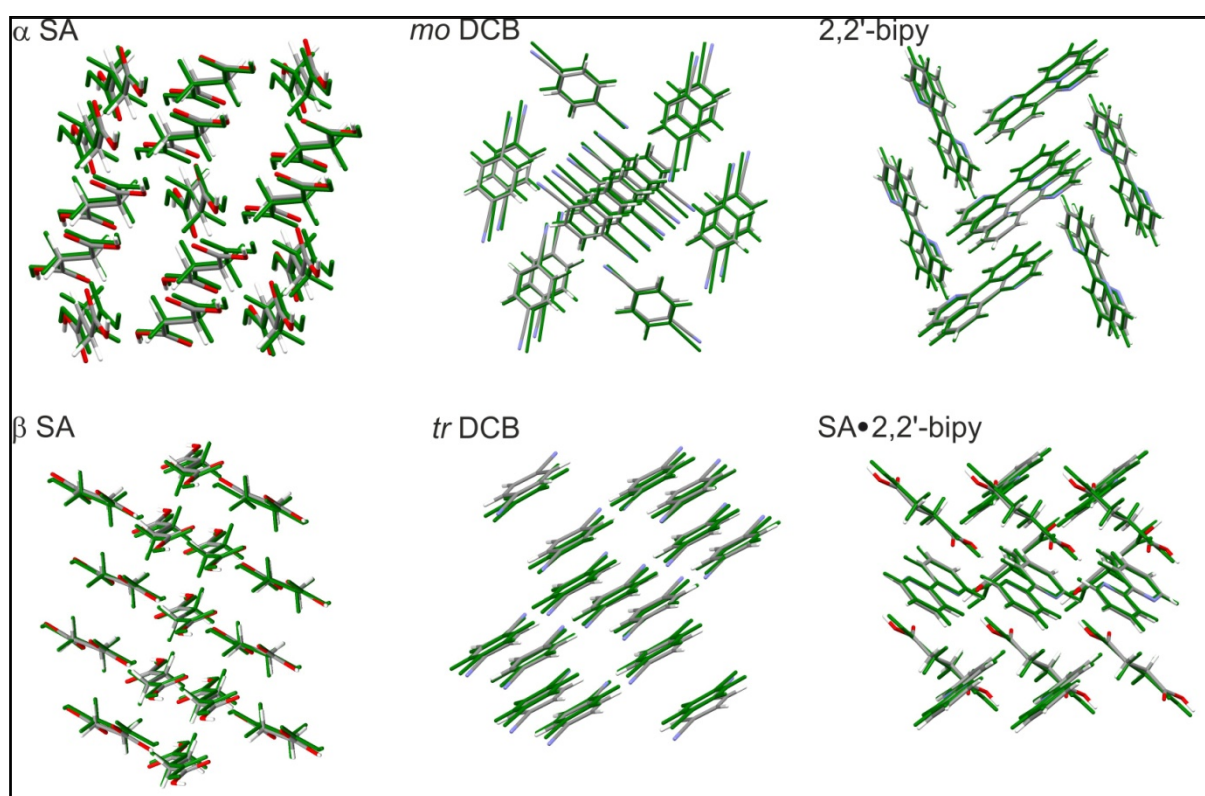


Figure S19. Overlay of the experimental (coloured by element) and the corresponding structures found in the search (green). *Mo* – monoclinic; *tr* – triclinic.